Chemical Physics Letters 468 (2009) 64–68

Contents lists available at ScienceDirect

Chemical Physics Letters

journal homepage: www.elsevier.com/locate/cplett

Enhancing light absorption and carrier transport of P3HT by doping multi-wall carbon nanotubes

Ming-Chung Wu [a], Yun-Yue Lin [a], Sharon Chen [a], Hsueh-Chung Liao [a], Yi-Jen Wu [a], Chun-Wei Chen [a], Yang-Fang Chen [b], Wei-Fang Su [a,c,*]

[a] Department of Materials Science and Engineering, National Taiwan University, No. 1, Section 4, Roosevelt Road, Taipei 106-17, Taiwan
[b] Department of Physics, National Taiwan University, Taipei 106-17, Taiwan
[c] Institute of Polymer Science and Engineering, National Taiwan University, Taipei 106-17, Taiwan

ARTICLE INFO

Article history:
Received 22 July 2008
In final form 25 November 2008
Available online 3 December 2008

ABSTRACT

We have investigated the enhancement of light absorption and carrier transport of poly(3-hexylthiophene) (P3HT) resulted from doping with multi-wall carbon nanotubes (MWNTs). The MWNTs were acid washed first, and then incorporated into P3HT homogenously. The MWNTs make P3HT unfolded with more alignment and thus increase light absorption as shown by the studies of AFM and UV–vis spectroscopy. The KFM data provides useful information to differentiate the work function of the MWNTs from P3HT and further show improved hole transporting behaviors. Based upon these results, the 0.01 wt% MWNTs doped P3HT/PCBM photovoltaic device shows an increase of 29% power conversion efficiency.

1. Introduction

Incorporating carbon nanotubes (CNTs) into conventional materials can potentially improve their inherent photochemical and mechanical properties and thermal stability [1–4], attributed to CNTs' large contact area, high dimensional aspect ratio and exceptional electrical conductivity. Especially, the nanotubes can be aligned during or after the composite fabrication by spin-casting, wet spinning, mechanical stretching, and melt fibre spinning [5–8]. Ikeda et al. reported a mechanochemical high-speed vibration milling technique to solubilize single-walled carbon nanotubes in organic solvents through the formation of complexes between the SWNTs and a polythiophene (PT) derivative [9]. The high aspect ratios of nanotubes exhibit many anisotropic properties, and those give better performance when they are aligned.

Recently, polymer solar cells have attracted a great interest in developing low-cost, large-area, and mechanically flexible photovoltaic devices [10–12]. The cell consists of donor/acceptor heterostructure which generates excitons upon sun light exposure. The excitons dissociate at the donor/acceptor interface to produce electrons and holes. Then, they move toward opposite electrodes to generate current. To reach a high efficiency, electron–hole dissociation and carrier transport rate play an important role [13–17]. Both single-walled carbon nanotubes (SWNTs) and multi-walled carbon nanotubes (MWNTs) have been found to enhance the conductivity of CNTs/polymer composites by many orders of magnitude [18–23]. With all the exceptional properties, CNTs can act as very good electron acceptors and exciton dissociation centres by providing high field at the polymer/CNT interfaces and further improve the device efficiency if integrated into polymeric photovoltaic devices. The merits of CNTs in photovoltaic devices often are, however, hindered by their tendency to aggregate and hamper homogenous film formation.

Samorì et al. [24] have reported that Kelvin probe force microscopy (KFM) is a powerful technique, not only for exploring electronic properties of materials, but also for optimizing the design and performance of new devices based on organic-semiconductor nanostructures. Hoppe et al. [25] reported KFM studies on MDMO-PPV (poly[2-methoxy-5-(3′,7′-dimethyloctyloxyl)]-1,4-phenylene vinylene)/PCBM (fullerene derivative 1-(3-methoxycarbonyl) propyl-1-phenyl-[6,6]C_{61}) films indicating that the lowering of the photocurrent of toluene cast samples came from hindered electron transport toward the cathode. At the same time, many studies also report that KFM can provide useful information for improving the photovoltaic performance, such as nanometer scaled work function and electronic transport behaviors [26,27].

Here, we report a simple technique to dope P3HT with MWNTs homogenously. The doped P3HT was characterized by AFM, UV–vis spectroscopy and Kelvin probe force microscopy. The doped P3HT exhibits enhanced light absorption and improved carrier transport behavior. We have further synthesized MWNTs doped P3HT/PCBM nanocomposites for photovoltaic device fabrication. The device shows an increase of 29% power conversion efficiency due to the fast carrier transport.

* Corresponding author.
E-mail address: suwf@ntu.edu.tw (W.-F. Su).

0009-2614/$ - see front matter © 2008 Published by Elsevier B.V.
doi:10.1016/j.cplett.2008.11.080

2. Experimental

2.1. Synthesis of HT–HT poly (3-hexylthiophene) and characterization

The HT–HT poly(3-hexylthiophene) was synthesized according to literature with some modifications [28]. 2,5-Dibromo-3-hexylthiophene (0.030 mol, 10 g) was added into a 500 ml three neck round bottom flask equipped with a 24/40 ground joint, a reflux condenser, and a magnetic stir-bar and was purged with dry nitrogen for 15 min. 320 ml freshly distilled tetrahydrofuran was transferred to the flask and the solution was stirred under dry nitrogen. The solution of tert-butylmagnesium chloride in diethyl ether (0.032 mol, 16 ml) was added via an airtight syringe and then heated in reflux for 1.5 h. The mixture was then allowed to cool to room temperature before adding Ni(dppp)Cl_2 (2 mol% of monomer, 0.33 g) and stirred at room temperature for 0.5 h. In order for the synthesized polymer to precipitate out, the solution was poured into 500 ml methanol. The solid was collected in a cellulose extraction thimble and then washed with methanol in a Soxhlet apparatus. The polymer was dried in vacuum overnight and gathered as a dark purple material (60% yield). The synthesized P3HT had an average molecular weight of M_w = 66 kDa with a polydispersity index (PDI) of 1.49 determined by GPC. ^{1}H NMR (400 MHz) result gave δ6.98 (s, 1 H), δ2.80 (t, 2 H), δ1.72 (pentet, 2 H), δ1.44 (m, 2 H), δ1.35 (m, 4 H), and δ0.92 (t, 3 H).

2.2. Preparation of multi-wall carbon nanotube solutions

Acid wash process was carried out to improve the MWNTs-polymer interaction and remove impurities. 5.00 g as-received multi-wall carbon nanotubes (MWNTs, DESUN nano company, Taiwan) was mixed with a total of 500.0 ml HNO_3: H_2SO_4 (volume ratio = 1:3) solution in a 3-neck round bottom flask. The mixture was stirred and heated to 80 °C and refluxed for 6 h. Water was used to dilute the solution (water: solution = 5:1 by volume) before it was filtered through a 0.2 μm-pore-sized PTFE filter disk. The filtered MWNTs were washed with excess water until the pH of the filtrate solution ~7.0 and then collected and dried in an oven. The dried MWNTs can be easily dissolved in 1,2-dichlorobenzene to prepare a 0.01 wt% solution.

2.3. Fabrication of P3HT–MWNTs nanocomposite thin films

The thin films were fabricated using the MWNTs solution and the synthesized P3HT prepared above. One master solution of 2.00 wt% P3HT and one master solution of 0.01 wt% MWNTs were separately prepared in 1,2-dichlorobenzene and mixed together in different compositions as needed. The mixed solution was sonicated for 30 min in a 70 kW sonicator in order to well disperse MWNTs. Different concentrations of MWNTs in P3HT hybrid solution, 0.01 wt%, 0.05 wt%, 0.10 wt%, 0.50 wt%, 1.00 wt%, were then prepared from two master solutions. After ultrasoned for 20 min, the hybrid solution was spin-coated onto indium–tin–oxide (ITO) glass substrate at 1000 rpm for 30 s. The ITO glass substrate with a sheet resistance of 15 Ω/square (Merck) was first ultrasonically cleaned in a series of organic solvents (ethanol, methanol and acetone).

2.4. Characterization of P3HT–MWNTs nanocomposite thin films

The MWNT microstructure was observed by a JEOL-100CX II (Japan) transmission electron microscope (TEM) operated at 100 keV. The film morphology was observed by atomic force microscopy (AFM) (Digital Instruments, Nanoscopes III). UV–vis absorption spectra were obtained using a Perkin Elmer Lambda 35 UV/VIS Spectrometer. The work function mapping was measured by Kelvin probe microscope (Digital Instruments, Nanoscopes III) in the dark or under illumination with halogen lamp (Royal Philips Electronics, 50 W).

2.5. Synthesis of MWNTs doped P3HT–PCBM solution

The P3HT and PCBM were blended in a 1:0.8 wt/wt ratio in 1,2-dichlorobenzene and stirred overnight at room temperature in the glove box. Then the MWNTs solution was added into the P3HT/PCBM solution and mixed under sonication for 30 min to prepare MWNT doped P3HT/PCBM solution.

2.6. Fabrication of MWNTs doped P3HT/PCBM and P3HT/PCBM photovoltaic devices

The ITO glass substrate was ultrasonically cleaned in a series of organic solvents (ethanol, methanol and acetone). A 40 nm thick layer of PEDOT:PSS (Baytron P, 4083) was spin-coated onto the ITO glass at 200 rpm for 10 s and 4500 rpm for 120 s consecutively to modify the ITO substrate surface. After baking at 120 °C for 30 min in the oven, the sample was transferred to a nitrogen filled glove box (<0.1 ppm for O_2 and H_2O) for active layer deposition. Two kinds of active layer materials: (1) P3HT/PCBM, (2) MWNTs doped (0.01 wt%) P3HT/PCBM, were spin-coated on the ITO glass at 700 rpm for 60 s. The thin film formed was then dried in a covered glass Petri-dish. Al electrode (~120 nm) was last deposited on the thin film by thermal evaporation. The performance of these devices was evaluated under AM 1.5G irradiation (100 mW/cm^2) using a solar simulator (Oriel Inc.).

3. Results and discussion

The MWNTs were examined under transmission electron microscopy (TEM) before and after acid treatment to observe their structural changes. The TEM photos are shown in the section of Supporting information. The pristine tubes illustrate continuous and smooth surface with an average diameter of 40–50 nm and an average length of 15 μm. After acid wash, the carbon nanotubes have disturbed outer surface and are much shorter and thinner than the ones before acid treatment. Atomic Force Microscope (AFM) was used to study the morphology and phase distribution of MWNTs doped P3HT samples. The 0.01 wt% MWNTs doped P3HT (Fig. 1a) exhibits a rough surface with small nodule-like structure, implying a large extent of continuous domains. Fig. 1b-e show a well dispersed MWNTs in P3HT and the morphology become smoother with increasing MWNTs contents. The high aspect ratios carbon nanotubes help the P3HT molecules to align along the nanotubes and form a more ordered structure. When the molecular chains are stretched out, the nodule-like structure gradually disappears and the surface morphology becomes smoother with the addition of MWNTs. It is interesting to note that we did not observe any increasing in surface roughness while increasing the MWNTs contents. The relatively short length and small diameter of acid treated MWNTs was homogenously dispersed in the polymer and stretched out the polymer molecules rather than self aggregated at high concentration [29].

The results of UV–vis absorption study of P3HT with various MWNTs concentration dopings are consistent with the AFM study. The P3HT molecules tend to be unfolded and aligned along the nanotubes, and ordered structure domains are formed. Fig. 2 shows that the absorption intensity of the vibronic structure becomes stronger with increasing MWNTs percentage, and these absorption spectra are normalized at 550 nm. The growing intensity in the spectrum corresponds to more ordered structures of P3HT molecules. The absorption spectra of the P3HT/PCBM system have been

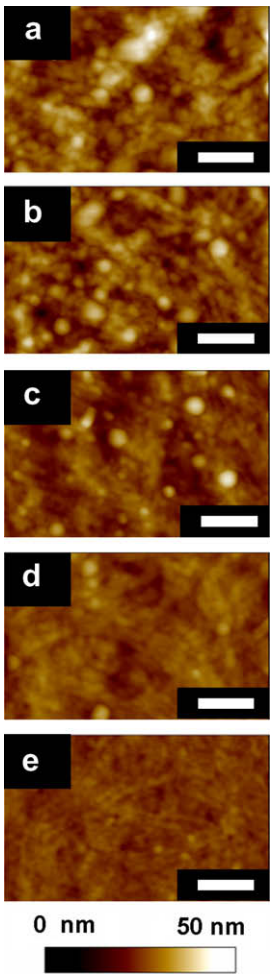

Fig. 1. AFM topographic images of P3HT with various concentration MWNTs doping. (a) 0.01 wt% MWNTs doped P3HT, (b) 0.05 wt% MWNTs doped P3HT, (c) 0.10 wt% MWNTs doped P3HT, (d) 0.50 wt% MWNTs doped P3HT, and (e) 1.00 wt% MWNTs doped P3HT. The scale bar is 200 nm.

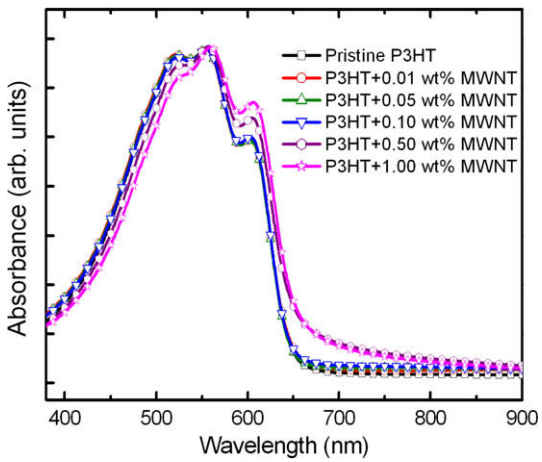

Fig. 2. UV–vis absorption spectra of P3HT with various doping concentration of multi-wall carbon nanotubes.

studied extensively. The PCBM does not increase the vibronic absorption of P3HT by simple mixing. However, the vibronic absorption of P3HT in the P3HT/PCBM composite can be enhanced by thermal annealing [30] or solvent annealing [31] as reported previously.

In order to understand the transport of carrier in the system, we employed KFM to investigate the work function of the film. For the purpose of comparison, we performed the work function mapping for P3HT/PCBM and P3HT/MWNTs systems, respectively. The KFM images for the P3HT/PCBM system are shown in Fig. 3. In a dark environment, the average value of the work function for P3HT-rich domain is 4.39 eV (light color regions in Fig. 3b), and for PCBM-rich domain is 4.44 eV (dark color regions in Fig. 3b). On the other hand, when the sample is measured under light illumination with halogen lamp, the measured work function values decrease for both of P3HT-rich domain (4.32 eV) and PCBM-rich domain (4.39 eV). Shifting to a lower work function value implies a growing electron cloud and relatively, decreasing in hole density. The negative behavior of PCBM induces a layer of hole around the clusters and results in a relatively small drop in the work function for PCBM-rich domain as compared to the P3HT-rich domain after light illumination [25].

Fig. 4 shows Kelvin probe force microscopy images of 0.10 wt% MWNTs doped P3HT film in the dark or under illumination. The Kelvin probe studies of pristine P3HT and MWNTs have shown their work function to be 4.64 and 4.91, respectively (The Kelvin probe microscope images of pristine P3HT and MWNTs and the discussion of the images are in the section of Supporting information.) Thus, the low work function of the light color regions in the KFM image is P3HT rich domain whereas the high work function of the dark color regions in the images is MWNTs rich domain. In the dark environment, the average value of work function for P3HT rich domain (light color regions in Fig. 4b) is 4.39 eV, and that for the MWNTs rich domain is 4.43 eV (dark color regions in Fig. 4b). When P3HT and MWNTs are mixed together, p–n junctions are formed in the film of the blend. The work function can be measured from the effective surface voltage of the sample by adjusting the voltage on the tip as the tip senses a minimum electric force from the sample. The sample contains the two components of P3HT and MWNTs that will show contrast due to differences in contact potential of each component. In the MWNTs/P3HT blend system, the decrease in work function of P3HT domain (from

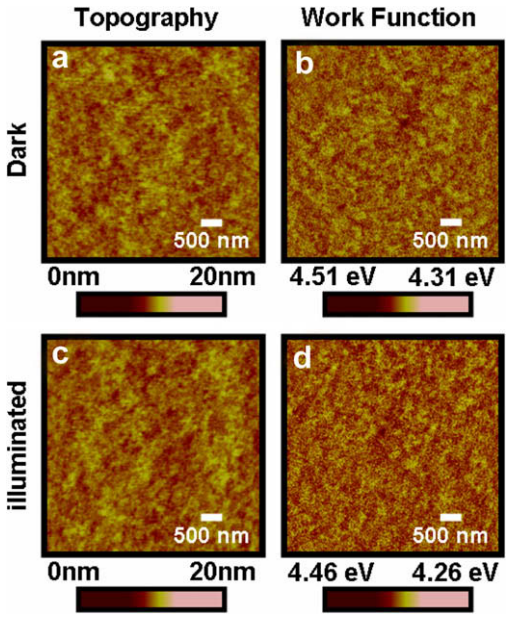

Fig. 3. Topography and work function of a blend film of P3HT/PCBM with a weight ratio of 1.0:0.8, measured in the dark and under illumination with halogen lamp. (a,b) are the topographic image and work function mapping image, respectively, taken in dark environment; (c,d) are the topographic image and work function mapping image, respectively, taken under illumination.

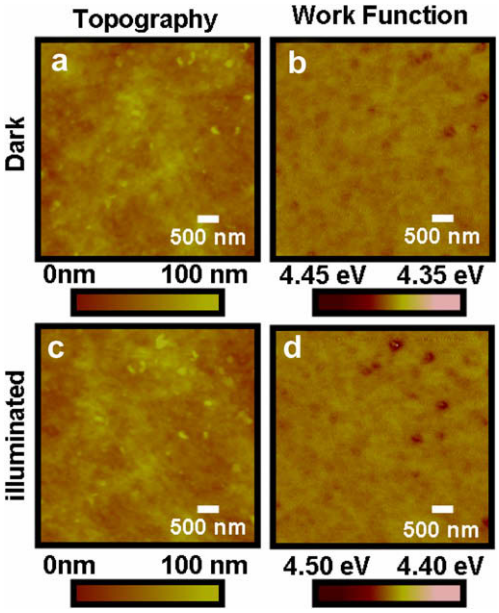

Fig. 4. Topography and work function of a blend film of 0.10 wt% MWNTs doped P3HT, measured in the dark and under illumination with halogen lamp. (a,b) are the topographic image and work function mapping image, respectively, taken in dark environment; (c,d) are the topographic image and work function mapping image, respectively, taken under illumination.

4.64 eV to 4.39 eV) is less than that of MWNT domain (from 4.91 eV to 4.43 eV). The work function of MWNT has to drop more to be 4.43 eV in order to have a balanced work function with a 4.39 eV of P3HT in the blend system. However, under light illumination, the average value of work function for P3HT rich domain has increased from 4.39 eV to 4.44 eV (light color regions in Fig. 4d), and that for the MWNTs rich domain has been increased from 4.43 eV to 4.48 eV (dark color regions in Fig. 4d). The positive shift of work function under light illumination corresponds to the enriched holes from MWNTs doping. The average work functions in P3HT/PCBM and P3HT/MWNTs system in the dark or under light illumination are summarized in Table 1.

We have fabricated solar cell from 0.01 wt% MWNTs doped P3HT/PCBM. Any concentration of MWNTs higher than 0.01 wt% gave non-functional solar cells due to the short-circuit caused by MWNTs. The thickness of the hybrid film was all controlled at 120 nm. Fig. 5 is the I–V characteristic curves of the solar cells measured under A.M. 1.5 illumination. MWNTs have been described as an interpenetrating electrode material that can extract holes of the polymer/PCBM layer easily [18,32–34], as shown in the inset. The MWNTs doped P3HT/PCBM solar cell shows an increase in the short-circuit current from 9.73 to 11.33 mA/cm^2 due to enhancement of light absorption and carrier transport. The incorporated MWNTs can help the hole transport and may reduce the possibility for electron–hole recombination, so the open-circuit voltage is increased from 0.50 to 0.52 V. As a result of increased short-circuit current and open-circuit voltage, the fill factor increases from 50.35% to 54.62% and the cell efficiency is improved from 2.69% to 3.47%. These data are summarized in Table 2. We can clearly observe an improvement of 29% power conversion efficiency when the cell is fabricated from the MWNTs doped P3HT/PCBM.

Table 1
The average work functions of P3HT/PCBM and P3HT/MWNTs system in the dark or under light illumination.

Materials		Work function (eV)	
		In the dark	Under light illumination
P3HT/PCBM	P3HT rich region	4.39	4.32
	PCBM rich region	4.44	4.39
P3HT/MWNTs	P3HT rich region	4.39	4.44
	MWNTs rich region	4.43	4.48

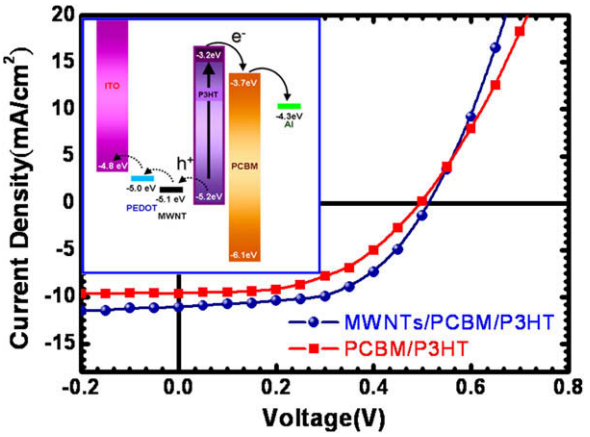

Fig. 5. I–V characteristic curves of solar cells measured under A.M. 1.5 illuminations. The cells are fabricated using PCBM/P3HT solar cell with and without MWNTs incorporation. The inset image shows energy levels of the single components of the photovoltaic cell for a ITO/PEDOT/P3HT:MWNTs:PCBM/Al device with MWNTs. The dashed and solid arrows indicate, respectively, hole and electron flows.

Table 2
Performance of P3HT/PCBM solar cell with and without MWNTs doping.

Samples	Voc (V)	Isc (mA/cm^2)	FF (%)	Power conversion efficiency (%)
P3HT/PCBM	0.50	9.73	50.35	2.69
P3HT/PCBM/MWNTs	0.52	11.33	54.62	3.47

4. Conclusions

We have demonstrated that acid washed MWNTs can be easily dispersed in the P3HT polymer matrix. The interaction between MWNTs and polymer facilitates the molecular organization of P3HT. The MWNTs forces the P3HT to be unfolded and aligned. We have observed an increased ordering in MWNTs doped P3HT from the studies of AFM and UV–vis spectroscopy. The KFM scanning differentiates the work function of the dopant from the polymer matrix and further implies the hole transport from the MWNTs within the system. The beneficial outcome of low-cost MWNTs doping in P3HT is clear and justified as shown in the improvement of solar cell performance. The device shows an increase of 29% power conversion efficiency due to the fast carrier transport.

Acknowledgements

This work is supported by National Science Council, Taiwan (Project No. NSC95-3114-P-002-003-MY3 and NSC96-2628-E-002-017-MY3) and the US Airforce Project (AOARD 074-014).

Appendix A. Supplementary data

Supplementary data associated with this article can be found, in the online version, at doi:10.1016/j.cplett.2008.11.080.

References

[1] A. Kongkanand, P.V. Kamat, ACS Nano 1 (2007) 13.
[2] P.M. Ajayan, J.M. Tour, Nature 447 (2007) 1066.
[3] J.A. Kim, D.G. Seong, T.J. Kang, J.R. Youn, Carbon 44 (2006) 1898.
[4] S. Wang, Z. Liang, T. Liu, B. Wang, C. Zhang, Nanotechnology 17 (2006) 1551.
[5] M. Moniruzzaman, K.I. Winey, Macromolecules 39 (2006) 5194.
[6] L. Jin, C. Bower, O. Zhou, Appl. Phys. Lett. 73 (1998) 1197.
[7] B. Safadi, R. Andrews, E.A. Grulke, J. Appl. Polym. Sci. 84 (2002) 2660.
[8] R. Haggenmueller, H.H. Gommans, A.G. Rinzler, J.E. Fischer, K.I. Winey, Chem. Phys. Lett. 330 (2000) 219.
[9] A. Ikeda, K. Nobusawa, T. Hamano, J. Kikuchi, Org. Lett. 8 (2006) 5490.
[10] W.U. Huynh, J.J. Dittmer, A.P. Alivisatos, Science 295 (2002) 2425.
[11] W. Ma, C. Yang, X. Gong, K. Lee, A.J. Heeger, Adv. Funct. Mater. 15 (2005) 1617.
[12] E. Perzon, F. Zhang, M. Andersson, W. Mammo, O. Inganös, M.R. Andersson, Adv. Mater. 19 (2007) 3308.
[13] T.W. Zeng, Y.Y. Lin, C.W. Chen, W.F. Su, C.H. Chen, S.C. Liou, H.Y. Huang, Nanotechnology 17 (2006) 5387.
[14] M. Graetzel, Nature 414 (2001) 338.
[15] Y.Y. Lin et al., J. Mater. Chem. 17 (2007) 4571.
[16] P. Wang, S.M. Zakeeruddin, J.E. Moser, M.K. Nazeeruddin, T. Sekiguchi, M. Grätzel, Nat. Mater. 2 (2003) 402.
[17] H.J. Snaith, M. Grätzel, Adv. Mater. 19 (2007) 3643.
[18] C. Li, Y. Chen, Y. Wang, Z. Iqbal, M. Chhowalla, S. Mitra, J. Mater. Chem. 17 (2007) 2406.
[19] A.D. Pasquier, H.E. Unalan, A. Kanwal, S. Miller, M. Chhowalla, Appl. Phys. Lett. 87 (2005) 203511.
[20] H. Hoppe, N.S. Sariciftci, J. Mater. Res. 19 (2004) 1924.
[21] T. Hasobe, S. Fukuzumi, P.V. Kamat, J. Phys. Chem. B 110 (2006) 25477.
[22] E. Kymakis, G.A. Amaratunga, J. Appl. Phys. Lett. 80 (2002) 112.
[23] B. Pradhan, S.K. Batabyal, A.J. Pal, Appl. Phys. Lett. 88 (2006) 093106.
[24] V. Palermo, M. Palma, P. Samorì, Adv. Mater. 18 (2006) 145.
[25] H. Hoppe, T. Glatzel, M. Niggemann, A. Hinsch, M.C. Lux-Steiner, N.S. Sariciftci, Nano Lett. 5 (2005) 269.
[26] T. Glatzel, M. Rusu, S. Sadewasser, M.C. Lux-Steiner, Nanotechnology 19 (2008) 145705.
[27] S. Sadewasser, T. Glatzel, S. Schuler, S. Nishiwaki, R. Kaigawa, M.C. Lux-Steiner, Thin Solid Films 431 (2003) 257.
[28] R.S. Loewe, S.M. Khersonsky, R.D. McCullough, Adv. Mater. 11 (1999) 250.
[29] J. Bouclé, S. Chyla, M.S.P. Shaffer, J.R. Durrant, D.D.C. Bradley, J. Nelson, Adv. Funct. Mater. 18 (2008) 622.
[30] F. Padinger, R.S. Rittberger, N.S. Sariciftci, Adv. Funct. Mater. 13 (2003) 85.
[31] G. Li, V. Shrotriya, J.S. Huang, Y. Yao, T. Moriarty, K. Emery, Y. Yang, Nat. Mater. 4 (2005) 864.
[32] S. Berson, R. Bettignies, S. Bailly, S. Guillerez, B. Jousselme, Adv. Funct. Mater. 17 (2007) 3363.
[33] J.Y. Kim, S.H. Kim, H.H. Lee, K. Lee, W. Ma, X. Gong, A.J. Heeger, Adv. Mater. 18 (2006) 572.
[34] H. Ago, H. Petritsch, M.S.P. Shaffer, A.H. Windle, R.H. Friend, Adv. Mater. 11 (1999) 1281.